Processing and Application of Ceramics 11 [4] (2017) 322–328
https://doi.org/10.2298/PAC1704322U

Thermomechanical properties of mullitic materials

Jan Urbánek[1,*], Jiří Hamáček[1], Jan Macháček[1], Jaroslav Kutzendörfer[1], Jana Hubálková[2]

[1]*Department of Glass and Ceramics, University of Chemistry and Technology, Prague, Technicka 5, CZ-16628 Praha 6, Czech Republic*

[2]*Institut für Keramik, Glas-und Baustofftechnik, Technische Universität Bergakademie Freiberg, Agricolastraße 17, 09599 Freiberg, Germany*

Received 7 May 2017; Received in revised form 8 November 2017; Accepted 6 December 2017

Abstract

Mechanical tests provide important information about the properties and behaviour of materials. Basic tests include the measurement of flexural strength and in case of refractory materials, the measurement of flexural strength at high temperatures as well. The dependence of flexural strength on the temperature of ceramic materials usually exhibits a constant progression up to a certain temperature, where the material starts to melt and so the curve begins to decline. However, it was discovered that ceramic mullitic material with a 63 wt.% of Al_2O_3 exhibits a relatively significant maximum level of flexural strength at about 1000 °C and refractory mullitic material with a 60 wt.% of Al_2O_3 also exhibits a similar maximum level at about 1100 °C. The mentioned maximum is easily reproducible, but it has no connection with the usual changes in structure of material during heating. The maximum was also identified by another measurement, for example from the progression of the dynamic Young's modulus or from deflection curves. The aim of this work was to analyse and explain the reason for the flexural strength maximum of mullitic materials at high temperatures.

Keywords: *mullitic materials, thermomechanical properties, flexural strength*

I. Introduction

Flexural tests (three-point, four-point) are used to study the mechanical properties of materials at room and elevate temperatures [1,2]. Many changes during heating of ceramic materials (for example the removal of physically and chemically bonded water, which is connected with the formation of pores, sintering, expansion/contraction, phase and chemical changes), are connected with the increasing or decreasing flexural strength. Thus, some processes can be recognised from the measurement of flexural strength at different temperatures. This measurement is also important because of the assessment of thermomechanical properties of materials and their utilization at high temperatures.

Changes in the material behaviour with rising temperature can also be observed by loading curves that represent the dependence of the strain of material on loading stress. They consist of the linear part, which corresponds with Hooke's law and can be followed by the nonlinear part [3,4]. The first part of the mentioned nonlinear part represents nonlinear reversible deformation, so after the interruption of material loading the deflection will come back to the zero point. However, if a certain stress is exceeded, an irreversible (plastic) deformation occurs. At normal temperatures, ceramic materials behave elastically according to Hooke's law and a shift of the crystal lattice as in the case of metals cannot be observed. At high temperatures, minor melting allows particles to move, thus material can exhibit plastic deformation as well.

The dependence of flexural strength on the temperature of fired aluminium silicates materials does not exhibit a significant increase or decrease of flexural strength up to high temperatures. At high temperatures, flexural strength decreases significantly due to the softening of the material and the formation of melt. An example of the dependence of flexural strength on the temperature can be seen in Fig. 1 for aluminium oxide. The same progression is also expected for fired mullitic materials, so their firing temperature is usually higher than the working temperature. Nevertheless, mullitic materials exhibit a maximum level of flexural strength at high temperatures.

*Corresponding authors: +420 220 444 149,
e-mail: *Jan.Urbanek@vscht.cz*

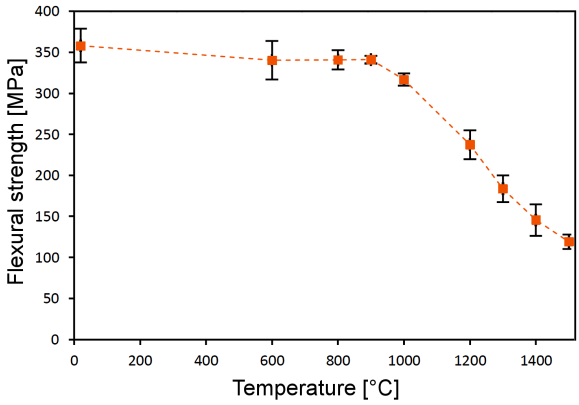

Figure 1. The dependence of flexural strength on the temperature of corundum material (Al_2O_3 content is 99.7 wt.% [5]

The aim of this work was to analyse and explain the presence of the maximum level of flexural strength of mullitic materials at high temperatures. The study was focused on structural changes in the material during heating and at high temperatures.

II. Materials and methods

2.1. Sample preparation

Two mullitic materials were chosen for studying thermomechanical properties: i) ceramic mullitic material (CMM) LUNIT 73 from ESTCOM CZ - Oxidová Keramika, a.s. and refractory mullitic material (RMM) A60S from P-D Refractories CZ a.s. The CMM was produced by mixing a powder of aggregates with binders and other additives in a ratio of Al_2O_3 : SiO_2 that corresponded to mullite. The resulting mass was extruded, dried and fired at 1700 °C to produce rods with diameter of 5 mm and length of 160 mm. The chemical and phase compositions of the material are given in Tables 1 and 2.

Table 1. Chemical composition determined by XRF analysis

Oxide	CMM content [wt.%]	RMM content [wt.%]
Al_2O_3	62.8	60.0
SiO_2	33.5	37.5
Fe_2O_3	0.8	1.0
TiO_2	0.5	0.3
$K_2O + Na_2O$	1.5+0.3	0.2+0.4
MgO	0.2	0.2
CaO	0.3	0.3
residue	0.9	0.1

Table 2. Pahse composition determine by XRD

Phase	CMM content [wt.%]	RMM content [wt.%]
mullite	99	85
corundum	1	7
andalusite		7
cristobalite		1

The refractory mullitic material (RMM) was used to produce refractory bricks, which are fired at 1500 °C. Their chemical and phase compositions are presented in Table 1 and 2. The prepared bricks were cut into the required samples for measurements.

2.2. Structural characterization

Samples for determination of chemical and phase compositions were prepared by grinding the CMM and RMM materials and pressing into a thin layer. The chemical composition was determined by ARL 9400 XP sequential WD-XRF spectrometer and results were evaluated by Uniquant 4 software. The phase composition was determined by X-ray diffractometer Panalytical - X'pert Pro and results were evaluated by the software Panalytical HighScore Plus 3.0e.

The broken samples were cut using a diamond disc saw, perpendicular to the fracture vertically and horizontally. They were photographed using a petrographic microscope (Nikon polarizing microscope Eclipse E400 Pol) with various enlargements using side lighting to highlight the cracks in the material.

2.3. Flexural strength

The determination of the flexural strength of CMM rods with a diameter of 5 mm and a length of 160 mm (Fig. 2) was done using a three-point arrangement. The material was first heated at a rate of 5 °C/min to the required temperature with a two-hour delay and then it was tested (broken) with a loading rate of about 15 N/s. The resulting flexural strength σ_F was calculated according to equation 1:

$$\sigma_F = \frac{8}{\pi} \cdot \frac{F_{max} \cdot l}{d^2} \tag{1}$$

where F_{max} is the force at which a sample was broken, l is the distance between supports and d is the diameter of the sample [6,7]. The dependence of flexural strength of the CMM material on temperature was measured three times.

The determination of the flexural strength of RMM blocks with a cross-section of 25 × 25 mm and length of 160 mm (Fig. 2) was done according to the norm EN 993-7. The RMM samples were tested in the same way as in the case of CMM. The resulting flexural strength

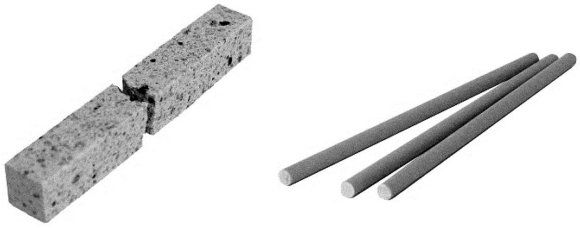

Figure 2. Tested RMM (left) and CMM (right) samples

σ_F was calculated according to equation 2 [7,8]:

$$\sigma_F = \frac{3}{2} \cdot \frac{F_{max} \cdot l}{b \cdot h^2} \tag{2}$$

where F_{max} is the force at which a sample was broken, l is the distance between supports, b is the width of a sample and h is the height of a sample. The deflection of the sample was recorded with a precision of 1 μm during its loading. The temperature was measured using a Pt-Rh thermocouple that was placed next to the pressure rod, about 1 cm above the specimen.

The dependence of flexural strength on temperature was measured five times. During measurement, the specimen deflection was recorded, and its progression was used for calculation of the static Young's modulus. The progression of the dynamic Young's modulus and damping with dependence on temperature was then measured using the impulse excitation technique.

2.4. Young's modulus

The dependence of the dynamic Young's modulus on temperature up to 1300 °C was determined using an impulse excitation technique, in which a sample is struck with a hammer and Young's modulus E is calculated from the captured frequencies:

$$E = 0.9465 \frac{m \cdot f_f^2}{b} \cdot \frac{L^3}{t^3} \cdot T_1 \tag{3}$$

where m is the mass of a sample, f_f is the primary resonant frequency, b is the width of a sample, L is the length of a sample, t is the thickness of a sample, T_1 is the correction factor for the fundamental flexural mode to account for the finite thickness of a bar, Poisson's ratio according to the norm ASTM E 1876-01 [7]. The specific damping Q was calculated from the progress of damping according to equation 4:

$$Q^{-1} = \frac{k}{\pi \cdot f} \tag{4}$$

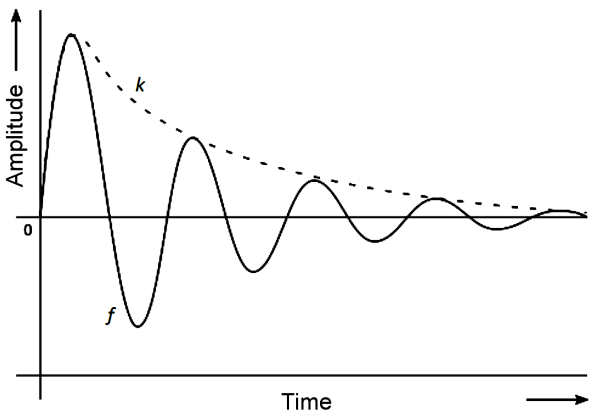

Figure 3. Damping of excited signal in material [10]

where k is the capacity of damping, which depends on the sample sizes and f is frequency [8,9]. The capacity of damping k was determined from the decrease of the excited signal, as you can see in Fig. 3 and equation 5:

$$A = e^{kt} \tag{5}$$

where A is amplitude and t is time [11].

III. Results

3.1. Structural characterization

The main difference between the CMM and RMM materials was their granulometry. The CMM was made of finer powder (particles size up to about 30 μm), because it is used to produce rods, tubes and capillaries with small thickness. Thus, on the fractured surface it was hard to distinguish individual particles. On the other hand, the RMM is used to produce bigger shaped products, and the fractured surface is much coarser and looked much more heterogeneous than the CMM. The orientation of the particles is random in both cases so we suppose the isotropic behaviour of the materials.

XRF analyses confirm that the ratio Al_2O_3 : SiO_2 in the CMM is equal to 65.2 : 34.8 wt.% what is somewhat lower in comparison to the theoretical ratio for mullite (71.8 : 28.2 wt.%). The determined Al_2O_3 : SiO_2 ratio in the RMM is even lower and is equal to 61.5 : 38.5%.

According to the determined phase composition it was obvious that almost 100% conversion of origin compounds to mullite was obtained in the CMM, whereas mullite content in the RMM was 85%. Residual phases represent the origin of unreacted compounds.

3.2. Flexural strength

Flexural strength of the CMM and RMM samples are presented in Fig. 4. The dependence of flexural strength on temperature of the CMM exhibits a significant maximum level at approximately 1000 °C. The dependence

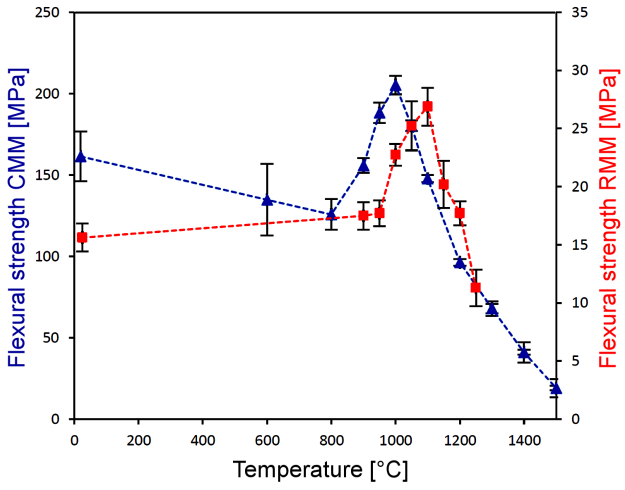

Figure 4. Dependence of flexural strength on the temperature of CMM (triangles) and RMM (squares)

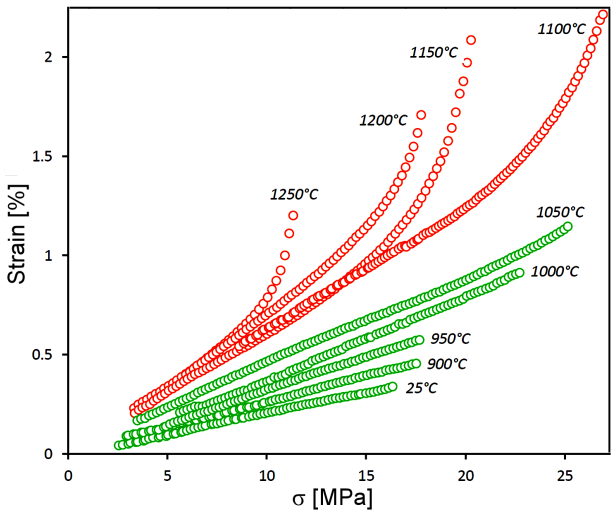

Figure 5. Stress-strain curves of RMM from 25 to 1250 °C that were gained during the determination of flexural strength

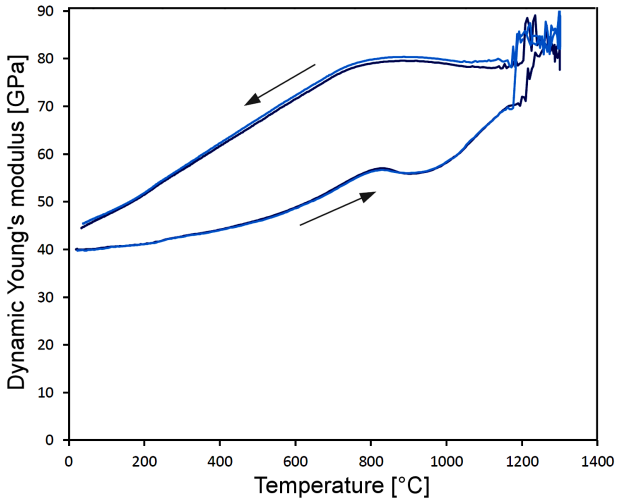

Figure 6. Dependence of the dynamic Young's modulus of RMM on temperature

of flexural strength on temperature of the RMM also exhibits a significant maximum level, but at somewhat higher temperature, i.e. at approximately 1100 °C.

3.3. Loading curves

The loading curves of the RMM in Fig. 5 were gained by choosing the loading curve which exhibits the closest bending strength as an average strength for each temperature. Up to 1000 °C, the curves only exhibit a linear progression, i.e. the elastic behaviour of the material. Above this temperature, the curves exhibit a non-linear part as well. The initial part of the curves was omitted because it contains a non-linear progression and many jump changes that are caused by connecting the compressive rod to the material during loading in flexure.

3.4. Young's modulus

The dependence of the dynamic Young's modulus exhibits hysteresis (Fig. 6). During heating, it exhibits a small local maximum and minimum, but above 1200 °C some noise can be observed. Measurement was repeated two times and the results were almost identical.

Damping with regard to temperature is negligible up to ~1000 °C. Above that value, the damping starts increasing and above ~1200 °C, it exhibits a large noise.

IV. Discussion

The chemical composition of both materials is relatively similar to mullite and the content of impurities is relatively low. The CMM exhibits a 1.2% higher content of alkaline oxides (Na_2O + K_2O) than the RMM. The higher content is intentionally modified to achieve better sintering activity of the material. Moreover, it probably corresponds to the lower maximum level of flexural strength of the CMM.

The CMM consists of 99% mullite and it points out its perfect transformation during firing, but the content of mullite in the RMM is 14% lower. The reason is probably the larger size of the aggregates in the RMM, which cannot be converted to the mullite. However, due to the semiquantitative character of the phase analysis, it is not possible to determine, how large a part is represented by amorphous compounds.

Both studied materials exhibit a maximum level of flexural strength at high temperatures (Fig. 4). The higher values of the flexural strength of the CMM material are caused by the finer structure and smaller size of the samples. The maximum level of the CMM is localized ~100 °C lower in comparison to the RMM. It is caused by the mentioned different amount of alkaline oxides. Due to the chemical and phase composition of both materials, which is similar to mullite, the mentioned maximum is not caused by chemical reactions at increased and high temperatures. Since the firing temperature is higher for both materials than the maximum of flexural strength (for CMM 1700 °C, so 700 °C higher than the temperature of the maximum, for RMM 1500 °C, so 400 °C higher than the temperature of the maximum), it cannot be attributed to sintering either.

Changes in the RMM during heating were studied using the dynamic Young's modulus, by damping and by progression of the loading curves with a dependence on temperature (Fig. 6). On account of the fact that the dependence of the dynamic Young's modulus on temperature exhibits hysteresis, the particles of aggregates probably have a different thermal expansion than the matrix [12]. Due to the shape and size of the hysteresis, the particles of the aggregates probably have larger thermal expansion than the matrix and hence they can be debonded from the surroundings at the laboratory temperature (25 °C). The local minimum of ~900 °C is probably caused by conditions, in which the debonded particles of aggregates are increased due to the increasing temperature to such a degree that they fill the space among them and the matrix and hence they form local tension with the further increasing temperature. The

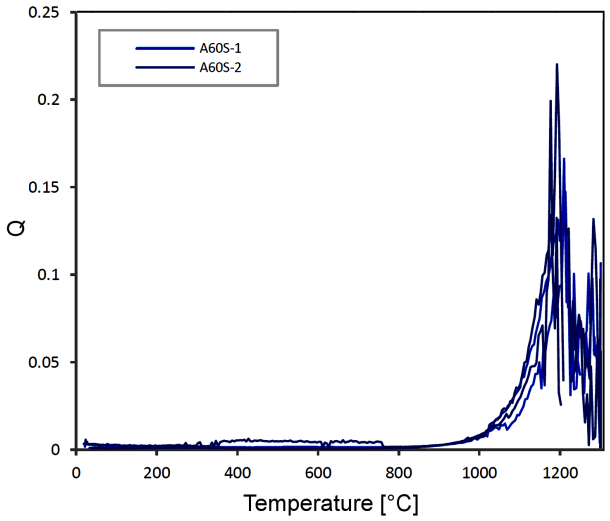

Figure 7. Dependence of damping on temperature of RMM

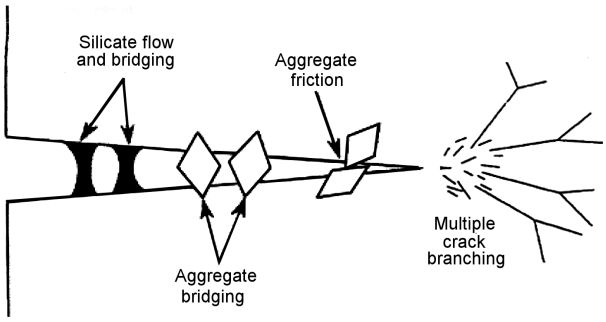

Figure 8. Processes, that absorb loaded energy during loading material [13]

regrowth of Young's modulus is probably caused by the softening of the material. It leads to the relaxation of tension and the healing of microcracks [13], which cause an increasing of flexural strength at high temperatures.

Above about 1000 °C, specific damping starts growing (Fig. 7), which is caused by an increased absorption of energy. Therefore, above this temperature, the material changes its microstructure, which corresponds to the softening of the material. It results in a higher value of flexural strength. This assumption is supported by the progression of loading curves with a dependence on temperature, which exhibits only a linear part up to approximately 1000 °C and above approximately 1050 °C they exhibit a non-linear part as well. At 1100 °C, i.e. at the temperature of the maximum level of flexural strength, the loading curve exhibits not only the largest value of loading, but also the largest value of specimen deflection. Therefore, there is a connection between the increasing of flexural strength and the plastic deformation of the material that allows the material to deflect without rupture. We can imagine the material as a system of solid particles of aggregates surrounded by a softened matrix or by a matrix containing a small amount of melt, which allows the plastic deformation under the load. The relationship between the aggregates and the matrix (for example the shape, strength of connection, surface, the temperature of softening and others) plays an important role in the extension of ruptures during loading, or in some cases may be in the strength of the material. For example, bigger shared surface between the aggregates and the matrix will lead to higher strength of the material, because the aggregate bridging (see Fig. 8) will make stronger connection of the rupture. On the other hand, bigger difference between thermal expansion of the aggregates and the matrix will lead to higher content of microcracks respectively debonding and so the strength will decrease.

Original and new ruptures are formed and grow during the loading of material in a three-point flexure. At the moment of critical rupture formation, a specimen breaks. Loaded energy to formation and the extension of ruptures can be absorbed by aggregate bridging, aggregate friction and melt bridging (Fig. 8) [14].

The first two processes are present in mullitic materials both at low and high temperatures. The third process is present just at high temperatures, when the material contains a small amount of melt and it increases the flexural strength. The presence of melt bridging is confirmed in Fig. 9a-c.

The softening of mullitic materials results in the relaxation of strain, healing microcracks, plastic deformation [15] and the presence of melt bridging during loading. It also results in an increase in flexural strength. The size of the strength increase, represented by the orange arrow in Fig. 10, depends on the chemical composition and material structure. Both studied materials exhibit the formation of microcracks by the difference expansion of the aggregate particles and matrix. How-

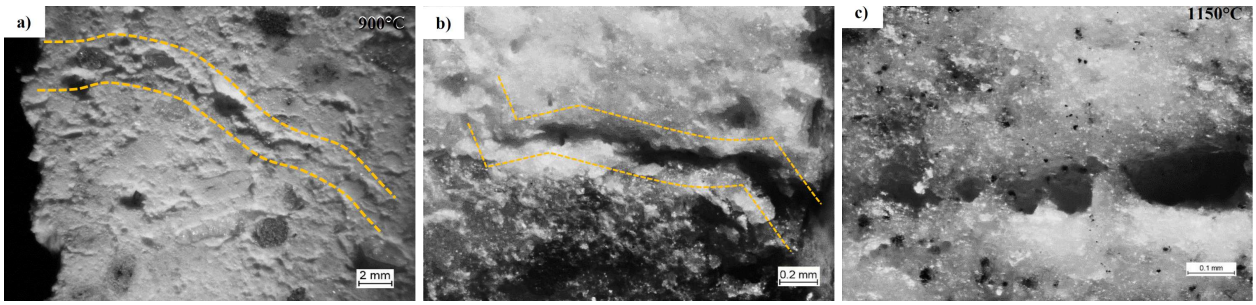

Figure 9. Cracks in the RMM after exposure to 900 °C and breaking during bending (a, b) - dash line curves serve as a guideline; and crack in the RMM containing bridges form a melt after exposure to 1150 °C and breaking in flexure (c)

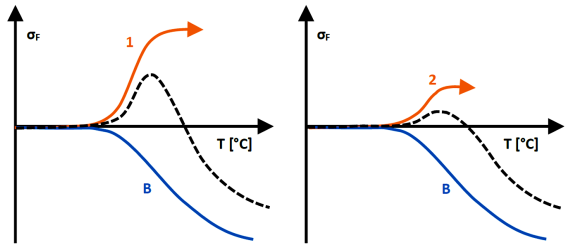

Figure 10. The influence of softening of material on the magnitude of flexural strength (the left graph represents material with higher numbers of microcracks at 25 °C; the blue curve represents the effect of growing temperature on decreasing viscosity; the orange curve represents the effect of softening; the black dotted curve represents the sum of two mentioned processes)

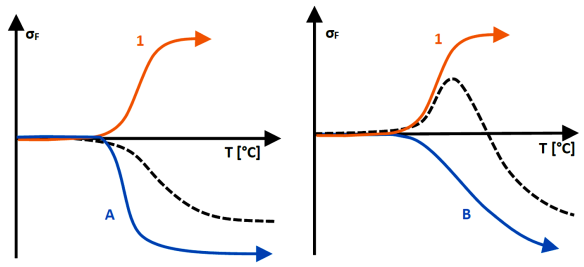

Figure 11. The influence of decrease of viscosity of material on the presence of a maximum of flexural strength (the blue curve represents the effect of growing temperature on decreasing viscosity; the orange curve represents the effect of softening on material; the black dotted curve represents the sum of two mentioned processes)

ever, since the RMM has a larger size of aggregate particles and a higher content of the compound with a different chemical composition, it exhibits a higher concentration of ruptures. Hence during heating and softening of the material, a higher number of ruptures are healed and a relatively higher increase of flexural strength occurs. The relative value of the RMM flexural strength maximum is about 7% higher than for the CMM.

However, there is a question, why, for example, Al_2O_3 does not exhibit a maximum level of flexural strength (Fig. 1), when it softens at a high temperature as well. The answer is a decrease of viscosity of the system (material can flow easily) that leads to a decrease in flexural strength (Fig. 11). If the positive effect of material softening prevails for a certain time, then the dependence of flexural strength exhibits the maximum level, as for example in the case of the studied mullitic materials. However, if the viscosity decreases faster at a short temperature interval, as in the case of Al_2O_3, then the decrease of viscosity predominates for all times and the material does not exhibit the maximum.

We can imagine it as perfectly sintered material that exhibits almost no healing of microcracks and the relaxation of strains with an increasing temperature. It softens and melts fast at quite a short temperature interval. So, although the softening of the material causes the formation of melt bridging and flexural strength should increase, the viscosity of the whole system is too low due to the quick formation of a larger amount of melt. So, the efficient of bridges on the increasing of flexural strength is low or zero, see Fig. 12. In case of mullitic materials, we suppose a slower decrease of viscosity with an increasing temperature (Fig. 12b), also due to the small amount of another component. We can imagine it as solid particles of aggregates surrounded by a relative plastic matrix.

A summary of the efficiency of the two mentioned actions and its influence on the presence of the flexural strength maximum at high temperatures is shown in graph from in Fig. 12.

V. Conclusions

Two mullitic materials were chosen for studying thermomechanical properties: i) ceramic mullitic material and refractory mullitic material. The fabricated mullitic materials exhibit the maximum of flexural strength at high temperatures, which is caused neither by chemical changes nor by the sintering. A study of microstructural changes with a dependence on temperature indicates the different thermal expansion of the presence aggregates and surrounding matrix, as well as the healing of microcracks and plastic deformation under the load at high temperatures. Therefore, the material can absorb energy in the formation and extension of ruptures during loading in flexure and it exhibits a higher deflection before its break. It results in higher values of flexural strength. On the other hand, the formation of a

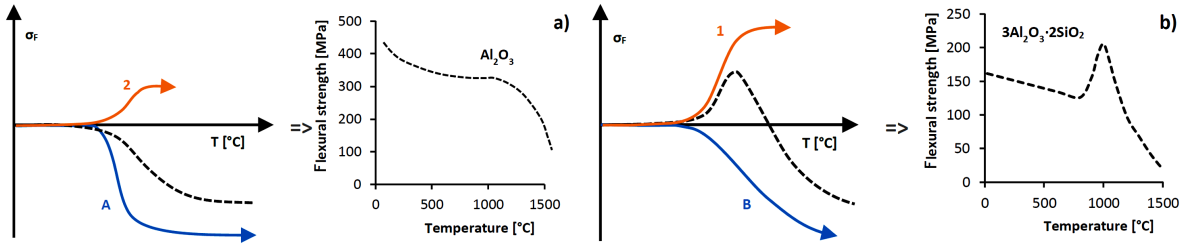

Figure 12. The connecting of two actions, which can cause the creation of the maximum level of flexural strength at high temperatures (the blue curves represent the effect of decreasing viscosity with growing temperature; the orange curves represent the effect of softening on material; the black dotted curves represent the sum of two mentioned processes): a) represents an example with no maximum - the case of corundum, b) represents an example with the maximum of flexural strength - the case of the tested mullitic materials

larger amount of melt causes the decrease of viscosity of the system and also a decrease of flexural strength. The balance between the material reinforcement (due to its softening) and decrease of viscosity (due to the formation of a larger amount of melt) determines the presence or absence of the flexural strength maximum at high temperatures. For example, in case of corundum material the presence of very low amount of microcracks and a quick decrease of viscosity at a high temperature lead to the absence of the maximum level of flexural strength at high temperatures. However, in case of the tested mullitic material, the healing of microcracks helps to increase the flexural strength and the formation of a plastic matrix with solid aggregates, which can absorb energy necessary for the formation and extension of ruptures during loading. This leads to an increase of flexural strength.

References

1. EN 993-6. - Methods of Testing for Dense Shaped Refractory Product - Part 6: Determination of Modulus of Rupture at Ambient Temperature, 1995.
2. EN 993-7. - Methods of Testing for Dense Shaped Refractory Products - Part 7: Determination of Modulus of Rupture at Elevated Temperatures, 1998.
3. J. Čulík, *Lineární Teorie Pružnosti*, Ústav biomedicínckého inženýrství, Mechanika, Czech Republic, www.fbmi.cvut.cz/e/pruznost/175.doc.
4. J.M. Gere, B.J. Goodno, *Mechanics of Materials*, Global Engineering, Cengage Learning, Canada, 2009.
5. J. Hamáček, *Private communication*, University of Chemistry and Technology, Prague.
6. F.P. Beer, R. Johnston, J.T. DeWolf, *Mechanics of Materials*, Fourth Edition in SI Units, The McGraw-Hill Companies, Inc., New York, NY, 2006.
7. ASTM E1876 - 15. Standard Test Method for Dynamic Young's Modulus, Shear Modulus, and Poisson's Ratio by Impulse Excitation of Vibration. 2005.
8. MANUAL RFDA HTVP1600 Version 2.2.1; IMCE N.V., Genk, Belgium.
9. G. Roebben, B. Bollen, A. Brebels, J. Biest, O. Biest, "Impulse excitation apparatus to measure resonant frequencies, elastic", *Rev. Sci. Instrum.*, **68** [12] (1997) 4511–4515.
10. A. Gajo, F. Cecinato, "Thermo-mechanical modelling of rock-like materials at a very high temperature: Application to ceramic refractories", *J. Eur. Ceram. Soc.*, **36** [9] (2016) 2193–2204.
11. N. Tessier-Doyen, J.C. Glandus, M. Huger, "Untypical Young's modulus evolution of model refractories at high temperature", *J. Eur. Ceram. Soc.*, **26** [3] (2006) 289–295.
12. R.C. Bradt, H. Harmuth, "The fracture resistance of refractories", *Refractories World Forum*, **3** [4] (2011) 129–132.
13. J. Hamáček, J. Macháček, J. Kutzendörfer, "Young modulus of refractories, measurements and data obtained", *Keramický Zpravodaj*, **28** [3] (2012) 9–11.
14. J. Werner, Ch.G. Aneziris, S. Dudczig, "Young's Modulus of elasticity of carbon-bonded alumina materials up to 1450 °C", *J. Am. Ceram. Soc.*, **96** [9] (2013) 2958–2965.
15. D.W. Richerson, *Modern Ceramic Engineering, Properties, Processing, and Use in Design*, CRC Press Taylor a Francis Group, LLC, 2006.